Proceedings of AVEC 2000
5th Int'l Symposium on Advanced Vehicle Control
August 22-24, 2000
Ann Arbor, Michigan

H_∞ CONTROL FOR INTEGRATED SIDE-SLIP, ROLL AND YAW CONTROLS FOR GROUND VEHICLES

Kazuya Kitajima[1] *Huei Peng*[2]
University of Michigan, Ann Arbor, MI, USA

Two integration algorithms for vehicle chassis control systems--a feedforward integration method and an H_∞ control algorithm, are designed and presented in this paper. Both integration methods aim to coordinate VDC, 4WS and active suspension functions of ground vehicle. The feedforward integration method is based on the idea of decoupling the control inputs and the control goals by rejecting the effects of other chassis control inputs. The H_∞ control algorithm minimizes a defined cost function under disturbances (driver's steering angle and braking) and design all the chassis control functions simultaneously. The performance of these two integration methods was compared against an un-coordinated control under a set of mild as well as severe driving maneuvers.

1. Introduction

Chassis control is important for vehicle safety. To enhance vehicle performance and reduce driving load, various types of chassis control systems have been developed in the last three decades, including ABS/traction control, 4WD, active suspension, 4WS, and VDC, many of which are now commercially available.

The inception of ABS systems came from attempts to prevent railcar wheel lock up in the early 1900s. For automobiles, ABS and traction control have evolved continuously since their introduction in the 1950s and 1980s, respectively (Mack 1996). ABS/traction control mainly affects vehicle longitudinal motion and acts independently on individual wheels to maintain tire braking and traction forces near their peak values. Various control design methods have been proposed, such as rule-based control algorithms (including fuzzy logic) (Mauer et al. 1994), sliding mode controller (Tan and Tomizuka 1990), etc.

Active suspensions generate additional forces to achieve improved performances. Main performance issues include (1) ride comfort, (2) tire/ground contact force, (3) suspension working space, and (4) vehicle attitude control. Various types of control methods have been applied to the design of active suspensions. Preview control is capable of improving rear suspension performance by measuring the road profile at the front wheels (Bender 1968). Optimal controls, especially LQ/LQG control design methods (Thompson 1976), are often applied in the design of active suspension systems. Active suspension system could affect longitudinal and lateral motions by controlling the distribution of the active roll moment between front and rear axles.

The main purposes of 4WS are (1) to reduce vehicle side slip angle, (2) to reduce the phase difference between yaw rate and lateral acceleration, and (3) to increase the lateral tire force reserve (force away from saturation). This system has two outputs (yaw rate and lateral velocity) and two inputs (front and rear steering angles). Consequently, yaw rate and side slip angle can be controlled independently. 4WS can reduce the vehicle side slip in the linear tire region. In an early work, Sano (1986) proposed an open loop control design to steer the rear wheels as a speed dependent function of the front wheel steering angle. Whitehead (1988) analyzed the use of yaw velocity feedback to determine rear wheel steering angle. A time delay is commonly introduced for the rear wheel steering angle (designed from static analysis) to improve stability and handling response. In several recent works, more sophisticated control methods have been applied to improve the performance of 4WS systems (Tagawa et al. 1996, Horiuchi et al. 1996, Ito et al. 1987).

Recently the Vehicle Dynamics Control (VDC) concept was proposed (Shibahata et al. 1992, Inegaki et al. 1994, Matsumoto et al. 1992). VDC systems directly controls yaw moment by generating differential longitudinal forces on left and right tires. From tire characteristics, longitudinal force usually has a margin to its saturation, even when lateral forces are near saturation. Under such conditions, controlling longitudinal tire forces is an effective way to influence vehicle yaw (and thus lateral) motions. VDC is applicable not only to passenger vehicles but also to trucks (Ma and Peng 1998). In order to describe the mechanism of vehicle behaviors with VDC in the nonlinear range, Shibahata et al. (1992) proposed a method showing the characteristics of yaw moment and side slip angle, which indicates that yaw moment is generated for reducing the vehicle side slip angle in the small side slip angle range, but the yaw moment declines in the large side slip angle range. Inagaki et al. (1994) suggested a phase plane method, which

[1] Graduate Student, currently with Metropolitan Expressway Public Corporation, Tokyo, Japan
[2] Associate Professor, corresponding author, hpeng@umich.edu

shows the relationship between side slip angle and its changing rate, to analyze vehicle dynamic stability in the nonlinear region. Phase plane methods require identification of stable and unstable regions in a large number of situations including different steering angles and speeds. Van Zenten (1996) proposed a yaw rate/side slip control design which requires estimating the desired yaw rate and side slip angle based on driver maneuvers instead of the phase plane. Several studies (Nagai et al. 1996, Shimada et al. 1994, Hirano et al. 1994, Abe et al. 1996) compared VDC with 4WS in terms of yaw rate model following, in terms of robustness to the longitudinal force, and confirmations of the effectiveness and performance limitation of 4WS and VDC have been reported.

A large number of control designs have been proposed for these vehicle motion control systems individually. However, the coordination/combination of these chassis control systems have not been amply discussed, even though some of these chassis controls have similar and/or complementary objectives. Moreover, since longitudinal, lateral, vertical forces and roll, pitch, yaw moments affect vehicle dynamics simultaneously, one chassis control may adversely influence the operations of other control systems. Thus, it is evident that appropriate integration of chassis controls could improve vehicle stability and safety.

This paper compares two integration design methods. The controlled vehicle is assumed to be equipped with actuators and sensors for active suspension, 4WS, and VDC to control side slip, roll, and yaw motions. In addition, the slip of all the four wheels are assumed to be regulated by ABS systems. The first integration design is a "feedforward integration" type. In this design, one vehicle control input is designated for each vehicle output and the others control inputs are treated as disturbances. This "primary control function" was assigned according to their relative authority ranks obtained from simulations. Control inputs are then determined so that the main control goals can be achieved while generating minimum disturbances to other systems. The second design is an H_∞ Control approach (Mianzo and Peng 1999), which optimizes the control inputs and goals with predictable disturbance. In this design, the front steering angle is considered as a detectable disturbance. In order to study the effectiveness of these two integration designs, a simulator, which realizes vehicle longitudinal, lateral, roll, yaw and each tire rotational motion, was developed. This simulator is also equipped with ABS/TCS, which is not included in the integrated chassis control design but nevertheless is active in maintaining slip ratio within an appropriate range independently. The simulation results are conducted according to a test matrix of near-emergency maneuvers such as rollover and spin out on normal as well as low friction surfaces. Both integrated-chassis control approaches are compared against the performance of un-coordinated design as well as the vehicle without chassis control.

2. Vehicle Modeling

The vehicle to be simulated is a Jeep Cherokee vehicle. We choose a SUV due to the fact that (1) it has a higher level of roll angle and thus the chassis control coordination is somewhat more complicated; and (2) the test data of this vehicle is available (Garrott et al. 1999) to validate our model. We developed a SIMULINK model with three masses: the sprung mass M_s, the front unsprung mass M_{uf}, and the rear unsprung mass M_{ur}. The sprung mass includes vehicle body and engine inertia. The unsprung masses include the wheel, axle, brake components, part of suspension systems, steering linkages and the transmission. The only degrees of freedom (DOF) of the two unsprung masses are the rotational motions of the wheels. In other words, the vehicle model has 8 DOF—longitudinal, lateral, yaw and roll of the vehicle sprung mass, and the rotational DOF of the four wheels. The development of the vehicle model is tedious but straightforward (see Kitajima 2000). Therefore, the equations are not presented in this paper.

The tire model used is the System Technology Inc. (STI) tire model (Allen et al. 1992). In this research, secondary effects such as camber thrust and aligning moment are ignored for the sake of simplicity. The longitudinal and lateral force characteristics were tuned against the test data published by VRTC (Garrott et al. 1999). The composite slip tire model (STIREMOD, Szotak 1988) was then used to obtain more accurate tire forces under combined slip. This model is based on a composite slip formulation with a quadratic function of longitudinal and lateral slip. A composite slip parameter, which is a function of tire slip angle and longitudinal slip ratio, is calculated. The composite slip is then used in a force saturation function with shaping parameters. From the force function, tire longitudinal and lateral forces are obtained. In order to translate the change in the peak coefficient of friction with different longitudinal and lateral force production, the coefficients of friction are modified based on a friction ellipse concept. Again, for details, please refer to (Kitajima 2000).

Figure 1 shows the comparison plot between the real test data and that of the simulation model. This test maneuver is a left J-turn of about 0.4g, at a speed of 11.1 m/sec (40km/hr). The simulated yaw rate, lateral acceleration and roll angle all match with the test data very well. Good correlation was also obtained under several other conditions, including those with higher speed (80km/hr) and/or at lower acceleration level (0.2g).

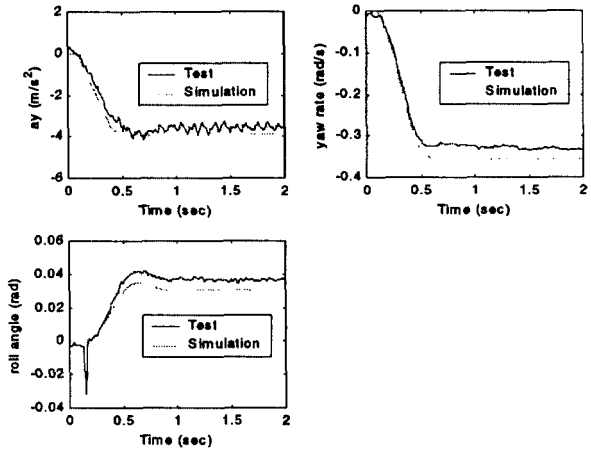

Figure 1 Model validation results (40km/hr, J-turn)

3. Un-Coordinated Control Algorithms

In order to benchmark the performance of the integrated chassis controller, an un-coordinated chassis controller, for which all four chassis control systems attempt to achieve their individual control goals without interaction, must be defined. These individual chassis controllers were designed to achieve certain control goals. In this research, the following chassis control designs are chosen to represent commonly designed algorithms.

3.1 VDC Controller

One of the main goals of VDC is to make the vehicle yaw rate, r, to track the desired yaw rate, r_d, which is estimated from the front steering angle and vehicle speed. The desired yaw rate is defined as follows:

$$r_d = \frac{u}{L(1+\frac{K_{us}}{L}u^2)}\delta_f \qquad (1)$$

where u is the forward speed, L is the wheelbase, K_{us} is the vehicle understeer coefficient and δ_f is the front wheel steering angle.

Another purpose of VDC is to limit the vehicle side slip angle β and side slip angle rate $\dot{\beta}$ to be within an acceptable region. In the phase plane of β and $\dot{\beta}$, these states might grow unbounded (spin-out) during a severe maneuver. Therefore, these states must be held near the origin of the phase plane by feedback controls. In order to achieve all the above mentioned goals, the following VDC control design (Van zanten et al. 1996) is applied:

$$T_{VDC} = C_{VDC1}|r - r_d| + C_{VDC2}|\beta + C_{VDC3}\dot{\beta}| \qquad (2)$$

Based on Equation (2), a differential braking torque is applied to the front wheels by increasing the braking pressure. When T_{VDC} is positive/negative, VDC activates the front left/right braking. The control gains (C_{VDC1}, C_{VDC2} and C_{VDC3}) were selected to be –480, -3200 and 1, respectively. The performance of this VDC controller under a 0.5Hz sinusoidal signal is shown in Figure 2. It can be seen that under this mild maneuver, the vehicle slip angle is reduced by about 15%.

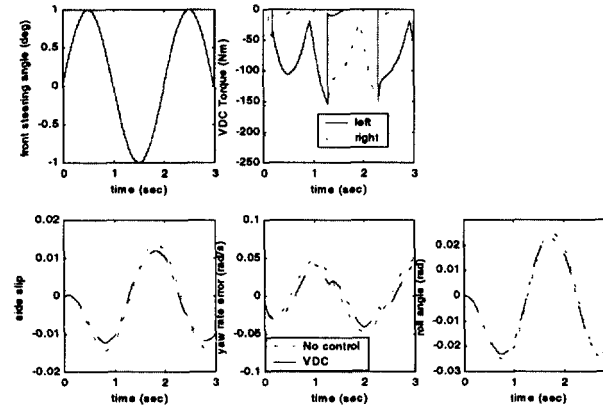

Figure 2 Performance of the VDC controller

3.2 4WS Controller

The main purpose of 4WS is to reduce vehicle side slip angle, or equivalently, vehicle lateral speed. For a linear 2 DOF bicycle mode, when the front and rear steering angles δ_f and δ_r are small, the lateral velocity and yaw moment are described by the following equation:

$$\begin{bmatrix}\dot{v}\\ \dot{r}\end{bmatrix} = \begin{bmatrix}\frac{-(C_{\alpha f}+C_{\alpha r})}{mu} & \frac{bC_{\alpha r}-aC_{\alpha f}}{mu}-u\\ \frac{bC_{\alpha r}-aC_{\alpha f}}{I_z u} & \frac{-(a^2C_{\alpha f}+b^2C_{\alpha r})}{I_z u}\end{bmatrix}\begin{bmatrix}v\\ r\end{bmatrix} + \begin{bmatrix}\frac{C_{\alpha f}}{m} & \frac{C_{\alpha r}}{m}\\ \frac{aC_{\alpha f}}{I_z} & \frac{-bC_{\alpha r}}{I_z}\end{bmatrix}\begin{bmatrix}\delta_f\\ \delta_r\end{bmatrix} \qquad (3)$$

where $C_{\alpha f}$ and $C_{\alpha r}$ are the cornering stiffness of the front and rear axles, respectively. A closed-loop control law (Whitehead 1988) for 4WS can be obtained from Eq.(3) by setting the lateral velocity v, and its derivative to zero. Thus we have:

$$\delta_r = \left(\frac{mu}{C_{\alpha r}} - \frac{b}{u} + \frac{aC_{\alpha f}}{uC_{\alpha r}}\right)r - \frac{C_{\alpha f}}{C_{\alpha r}}\delta_f \qquad (4)$$

In other words, the rear steering angle is determined from the front steering angle and yaw rate. The performance of this 4WS controller under a 0.5Hz sinusoidal signal is shown in Figure 3. Both slip angle and roll angle is reduced, at the expense of a more understeered vehicle.

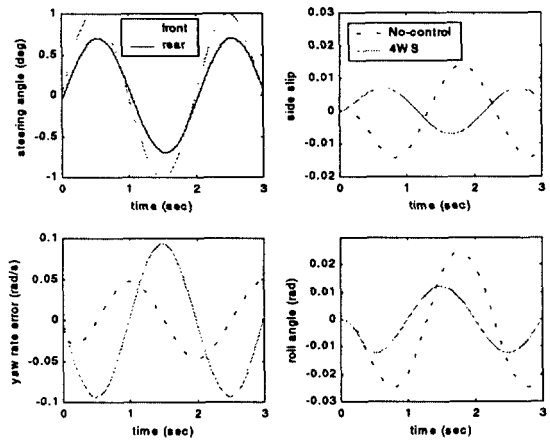

Figure 3 Performance of the 4WS controller

3.3 Active Suspension Controller

As mentioned previously, this research focuses on vehicle stability rather than non-critical issues such as ride comfort. Thus the purpose of the active suspension is to maintain a small roll angle. A PID control is applied to achieve the goal, and the active roll moment is calculated from:

$$M_{AS} = -K_p\left(1+\frac{1}{T_I s}\right)\phi \qquad (5)$$

where ϕ is the vehicle roll angle and the control gains are K_p=5000 and T_I=0.1. Under a step steering (Figure 4), the AS controller reduces the steady-state roll angle to zero, and has very little effect on vehicle handling variables such as yaw rate.

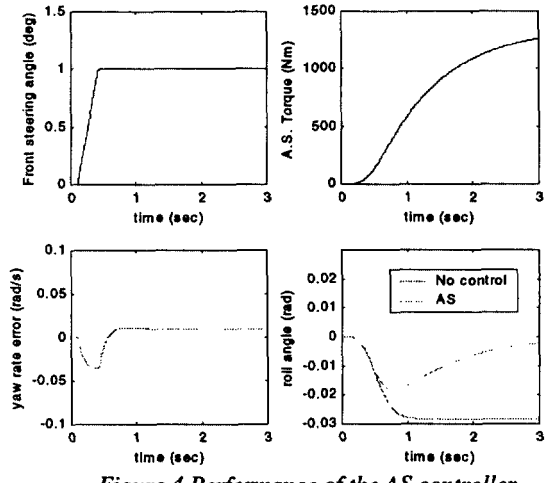

Figure 4 Performance of the AS controller

3.4 ABS/Traction Controller

The ABS/Traction controller is not included in the final chassis integration. However, it is assumed to exist and could interfere with the operation of other chassis control functions. A standard rule-based algorithm with perfect slip measurement is used. The ABS/Traction algorithm is assumed to generate a traction/brake torque, which maintains tire slip within a range. Specifically, the control algorithm is

If $|S_x| < |S_{x\min}|$

$$\Delta T_{A/T}(k) = sign(S_x)\times C_{A/T1}(|S_{x\min}| - |S_x|)\times|T_x(k-1)| \qquad (6)$$

If $|S_x| > |S_{x\max}|$

$$\Delta T_{A/T}(k) = -sign(S_x)\times C_{A/T2}(|S_x| - |S_{x\max}|)\times|T_x(k-1)| \qquad (7)$$

where the control gains are chosen to be $C_{A/T1}$=2 and $C_{A/T2}$=2. Finally, the wheel torque is simply the summation of the driver-applied torque, VDC-applied torque, and the ABS/Traction torque:

$$T_x = T_{drv} + T_{VDC} + \Delta T_{A/T} \qquad (8)$$

4. Integrated Chassis Controllers

Chassis control functions interact with each other throughout their influence on vehicle's states. For instance, when the VDC is activated, it changes the longitudinal speed, yaw rate, and lateral velocity, which then influences the effectiveness of 4WS. Furthermore, VDC influences tire lateral forces, and thus impacts the function of active suspension. Moreover, VDC is essentially a braking operation; therefore, an interaction exists between VDC and ABS. Obviously, it is important to integrate controllers to achieve desired vehicle performance.

4.1 Feedforward Integration

One intuitive integrated chassis control design comes from the concept of "relative authority". A chassis control function (i.e., VDC) affects the control goal (i.e., yaw rate) to a relatively greater degree than other vehicle states (i.e., side slip, roll angle, slip ratio). Therefore, we can designate main objective to each chassis controller and treat other control inputs as disturbances. In general, the main goal of 4WS is to reduce vehicle side slip. Hence, other inputs (VDC, active suspension) are viewed as disturbances. Similarly, the main objective of active suspension is to control the roll angle. Finally, VDC manages the difference between the yaw rate and the desired yaw rate. For yaw rate, therefore, 4WS and active suspension inputs are disturbances.

A linearized vehicle model can be used to obtain vehicle transfer functions, based on which the decoupled algorithm can be developed. The linear 3-DOF yaw-roll model used is as following:

$$\begin{bmatrix} M & 0 & M_s h & 0 \\ 0 & I_{zz} & I_{xz} & 0 \\ M_s h & I_{xz} & I_{xx} & 0 \\ 0 & 0 & 0 & 1 \end{bmatrix} \begin{bmatrix} \dot{v} \\ \dot{r}-\dot{r}_d \\ \dot{p} \\ \dot{\phi} \end{bmatrix} =$$

$$\begin{bmatrix} -\frac{C_{\alpha f}+C_{\alpha r}}{u} & \frac{bC_{\alpha r}-aC_{\alpha f}}{u}-Mu & 0 & 0 \\ \frac{bC_{\alpha r}-aC_{\alpha f}}{u} & -\frac{a^2C_{\alpha f}+b^2C_{\alpha r}}{u} & 0 & 0 \\ 0 & M_s hu & -K_p & M_s gh-K_\phi \\ 0 & 0 & 1 & 0 \end{bmatrix} \begin{bmatrix} v \\ r-r_d \\ p \\ \phi \end{bmatrix}$$

$$+\begin{bmatrix} C_{\alpha r} & 0 & 0 \\ -bC_{\alpha r} & \frac{T_f}{2R_w} & 0 \\ 0 & 0 & 1 \\ 0 & 0 & 0 \end{bmatrix} \begin{bmatrix} \delta_r \\ T_{VDC} \\ M_{AS} \end{bmatrix} + \begin{bmatrix} C_{\alpha f}-\frac{u}{L(1+\frac{K_{us}}{L}u^2)}\left(\frac{bC_{\alpha r}-aC_{\alpha f}}{u}-Mu\right) \\ aC_{\alpha f}-\frac{u}{L(1+\frac{K_{us}}{L}u^2)}\left(-\frac{a^2C_{\alpha f}+b^2C_{\alpha r}}{u}\right) \\ -\frac{u}{L(1+\frac{K_{us}}{L}u^2)}(-M_s hu) \\ 0 \end{bmatrix} [\delta_f] \tag{9}$$

where the desired yaw rate r_d is assumed to be constant. The forward speed u is treated not as a variable but a parameter. After applying the Laplace transformation and setting δ_f to zero, Equation (9) can be reduced to:

$$\begin{bmatrix} C_{\alpha f}+C_{\alpha r}+Mus & \frac{bC_{\alpha r}-aC_{\alpha f}}{u}+M & M_s hs^2 \\ aC_{\alpha f}-bC_{\alpha r} & \frac{a^2C_{\alpha f}+b^2C_{\alpha r}}{u}+sI_{xz} & s^2I_{xz} \\ M_s hus & M_s hu+sI_{xz} & K_\phi-M_s gh+sK_p+s^2I_{xz} \end{bmatrix} \begin{bmatrix} \beta \\ r-r_d \\ \phi \end{bmatrix} = \begin{bmatrix} C_{\alpha r} & 0 & 0 \\ -bC_{\alpha r} & \frac{T_f}{2R_w} & 0 \\ 0 & 0 & 1 \end{bmatrix} \begin{bmatrix} \delta_r \\ T_{VDC} \\ M_{AS} \end{bmatrix}$$

Or,

$$g_1(s)\begin{bmatrix} \beta \\ r-r_d \\ \phi \end{bmatrix} = g_2 \begin{bmatrix} \delta_r \\ T_{VDC} \\ M_{AS} \end{bmatrix} \tag{10}$$

In order to make each control input only affect its main objective (i.e., β is affected only by δ_r etc.), we could design a transformation matrix F(s) such that

$$\begin{bmatrix} \beta \\ r-r_d \\ \phi \end{bmatrix} = G(s)\begin{bmatrix} \delta_r \\ T_{VDC} \\ M_{AS} \end{bmatrix} = G(s)F(s)\begin{bmatrix} \delta_r^o \\ T_{VDC}^o \\ M_{AS}^0 \end{bmatrix} = \begin{bmatrix} G_{11}(s) & 0 & 0 \\ 0 & G_{22}(s) & 0 \\ 0 & 0 & G_{33}(s) \end{bmatrix} \begin{bmatrix} \delta_r^o \\ T_{VDC}^o \\ M_{AS}^0 \end{bmatrix}$$

where $G(s) = g_1^{-1}(s)g_2$ and

$$F(s) = G(s)^{-1}\begin{bmatrix} G_{11}(s) & 0 & 0 \\ 0 & G_{22}(s) & 0 \\ 0 & 0 & G_{33}(s) \end{bmatrix} \tag{11}$$

is the matrix which decouples the effect of the three input signals. Through simulation verifications, we found that the decoupling matrix obtained from the vehicle transfer function does not work very well. The main reason, we believe, is due to the fact that transfer functions are based on linear models and thus accurately predict vehicle behavior only under small input amplitudes. Chassis control functions, on the other hand, are important under large inputs. Therefore, we decided to design the decoupling matrix by using step response results. For example, the (1,1) element of the G matrix can be obtained from the steady-state response of β under a rear wheel steering input, and so forth. The "experimentally" obtained matrix was found to be

$$G_{\exp}(0) = \begin{bmatrix} 2.15 & -1.8\times10^{-5} & 0 \\ -7.59 & 1.1\times10^{-4} & 0 \\ 1.43 & -2.05\times10^{-5} & 2.1\times10^{-5} \end{bmatrix}$$

Consequently, the decoupling matrix is

$$F_{\exp}(0) = \begin{bmatrix} 2.37 & 1.98\times10^{-5} & 0 \\ 1.63\times10^{5} & 2.37 & 0 \\ -1.75\times10^{3} & 0.96 & 1 \end{bmatrix}$$

This matrix will be used to modify the un-coordiated control signals presented in Section 3, to achieve a "feedforward" based decoupled response.

4.2 H_∞ Integration

The second integrated chassis control method studied in this research is the H_∞ control algorithm. The front steering angle is measured and is regarded as a disturbance input, whose effect is to be rejected by the control signal. In practice, there exists a delay from the time the driver turns the steering wheel to the time when the tire slip angle is generated. Thus, it is possible to take advantage of this delay as preview (information. In this research, however, the front steering angle is only used as the feedforward control information (i.e., preview time=0) for sake of simplicity. To design the H_∞ controller, we also need a linear model. Eq.(9) is used as the basis of the linear model, which is rewritten as

$$M'\dot{x} = A'x + B_1'w + B_2'u + B_p'w_p \tag{12}$$

where w is the lumped, non-previewable disturbance term, $x = [v \;\; r \;\; p \;\; \phi]^T$ is the state vector, $u = [\delta_r \;\; T_{VDC} \;\; M_{AS}]^T$ is the control vector and $w_p = \delta_f$ is the previewable disturbance. The matrix B_1' can be selected based on plant uncertainties w. Eq.(12) can then be rewritten as

$$\dot{x} = Ax + B_1 w + B_2 u + B_p w_p \tag{13}$$

The output vector to be penalized is

$$z = \begin{bmatrix} v \\ a_y - a_{y_d} \\ \phi \\ \alpha_r \\ T_{VDC} \\ M_{AS} \end{bmatrix} = C_1 x + D_{11}w + D_{12}u + D_{1p}w_p \tag{14}$$

The first three elements represent the control objective in minimizing vehicle side-slip, achieving good yaw following, and reducing roll angle. The last three elements in z represent the objective in using control signals frugally.

Following the procedure of H_∞ preview control algorithms (Mianzo and Peng 1999), the optimal control law under zero preview time is

$$u(t) = (g_1 + g_3 P)x(t) + g_2 w_p(t) \tag{15}$$

where $g_1 = \Pi_1(D_{12}^T C_1 + D_{12}^T D_{11}\Delta_2 D_{11}^T C_1)$, $g_3 = \Pi_1(D_{12}^T D_{11}\Delta_2 B_1^T + B_2^T)$ and $g_2 = \Pi_1(D_{12}^T D_{11}\Delta_2 D_{11}^T D_{1p} + D_{12}^T D_{1p})$. The matrices $\Delta_2 = (\gamma^2 - D_{11}^T D_{11})^{-1}$ and $\Pi_1 = -(I + D_{12}^T D_{11}\Delta_2 D_{11}^T D_{12} + D_{12}^T D_{12})^{-1}$ are solved from system state space matrices. The feedback gain matrix P is solved from the Riccati equation

$$\frac{dP}{dt} + P\alpha - P\beta P - \chi - \delta P = 0 \quad P(t_f) = 0 \qquad (16)$$

by using Algebraic Riccati Equation solvers such as the MATLAB are() command ($P = are(\alpha, -\beta, -\chi)$).

Additional matrices needed to solve the feedback matrix P are defined as following:

$$\begin{aligned}
\alpha &= A + B_1\Pi_2(D_{11}^T C_1 + D_{11}^T D_{12}\Delta_1 D_{12}^T C_1) \\
&\quad + B_2\Pi_1(D_{12}^T C_1 + D_{12}^T D_{11}\Delta_2 D_{11}^T C_1) \\
\beta &= -B_1\Pi_2(D_{11}^T D_{12}\Delta_1 B_2^T + B_1^T) - B_2\Pi_1(D_{12}^T D_{11}\Delta_2 B_1^T + B_2^T) \\
\chi &= \gamma^2 g_4^T g_4 - g_1^T g_1 - \Pi_3 C_1 - \Pi_3 D_{11} g_4 - \Pi_3 D_{12} g_1 \\
\delta &= \gamma^2 g_4^T g_6 - A^T - \Pi_3 D_{11} g_6 - \Pi_3 D_{12} g_3 - g_1^T g_3 - g_1^T B_2^T - g_4^T B_1^T \\
g_4 &= \Pi_2(D_{11}^T C_1 + D_{11}^T D_{12}\Delta_1 D_{12}^T C_1) \qquad (17) \\
g_6 &= \Pi_2(D_{11}^T D_{12}\Delta_1 B_2^T + B_1^T) \\
\Pi_2 &= (\gamma^2 - D_{11}^T D_{12}\Delta_1 D_{12}^T D_{11} - D_{11}^T D_{11})^{-1}
\end{aligned}$$

Since the preview time is assumed to be zero, the equations to solve preview gains are not presented in this paper.

5. Simulation Matrix

To evaluate the performance of vehicles with/without chassis controls, various test maneuvers have been proposed. The maneuvers selected for this study are similar to the maneuvers used in a NHTSA report (Garrott et al. 1999). The primary maneuvers are variations of J-turn and fishhook maneuvers. The J-turn maneuver excites vehicle roll and spin motions and simulate vehicle behavior under sudden turns onto a sharp ramp. In this maneuver, the vehicle starts in a straight line. At the time 0.0(s), the driver steers the handwheel from 0 to 330 degrees within 0.33(s). Figure 5 shows this steering angle as a function of time. The fishhook maneuver attempts to induce two-wheel lift-off by suddenly making a drastic turn and then turning back even further in the opposite direction. As shown in Figure 5, the driver steers the handwheel from 0 to approximately -123 degrees (-7.5 degrees times steering ratio 16.36) during the first 0.25(s). After maintaining the steering angle for 0.5(s), the driver turns the handwheel to the opposite direction to 600 degrees within 1.4(s) and maintains the angle for the remainder of the maneuver. This is the "fishhook-2" maneuver described in (Garrott et al. 1999).

In the second group of maneuvers, the brake action is included. In the braking-in-a-J-turn maneuver, pulse braking is applied between 1.33(s) and 1.83(s). The braking torques are -900(Nm) at front and -600(Nm) at rear tires. The timing of the brake torque is shown in Figure 5. Another scenario is the low friction case. The low-friction condition changes the coefficients in the STI tire model within the braking in a J-turn maneuver. For tuning the chassis control gains, a J-turn with a smaller steering wheel angle and a sinusoidal steering maneuver (Figure 6) is employed based on which the chassis control gains are tuned.

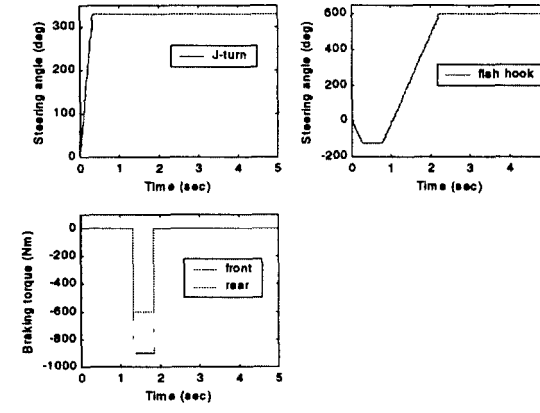

Figure 5 J-turn, Fishhook and braking inputs

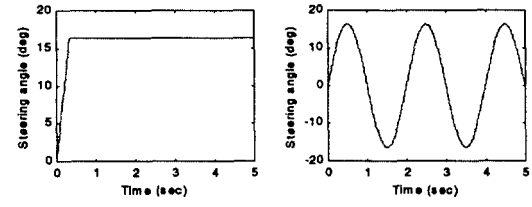

Figure 6 Small J-turn and Sinusoidal maneuvers

6. Simulation Results

In this chapter, simulation results of (1) a vehicle without chassis controls, (2) a vehicle with un-coordinated controls, (3) a vehicle with the feedforward integration, and (4) a vehicle with the H_∞ integration controller, under the simulation matrix scenarios are presented in the previous section.

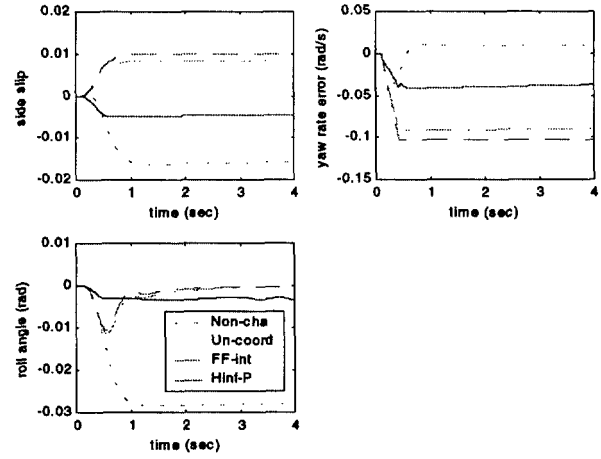

Figure 7 Vehicle response under small J-turn maneuver

Figure 7 shows the three main vehicle response signals (the main control goals) under the small J-turn maneuver. As can be seen, the H_∞ control is the most effectively. In terms of roll angle, all the controllers decrease the value drastically. However, this improvement is achieved at the expense of more understeered response.

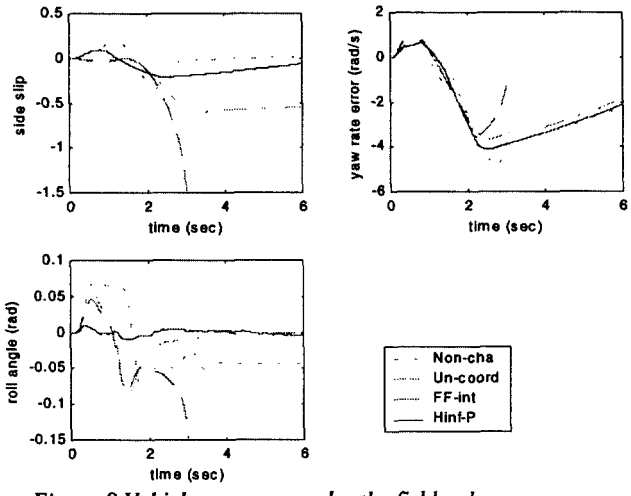

Figure 8 Vehicle response under the fishhook maneuver

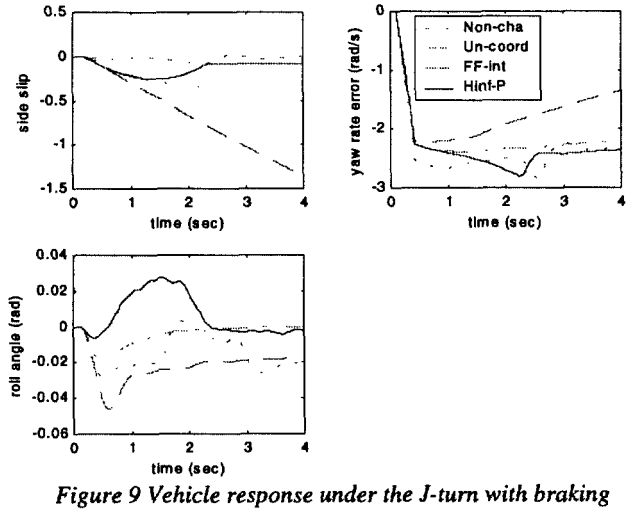

Figure 9 Vehicle response under the J-turn with braking

Figure 8 shows the main vehicle response under the fishhook maneuver. It is obvious that the feedforward integration method fail to work properly. This again is due to the fact that the feedforward decoupling is based on rejecting other controls' effect, regardless of whether these controls are "good" or "bad". Due to the saturation limits of control signals, such "reject both good and bad disturbances" concept reach into nonlinear regions and thus fail to work. Overall, the H_∞ algorithm works the best with significantly lower side slip. Figure 9 shows the results under the J-turn with braking (low-mu) maneuver. Again, the feedforward integration algorithm fail to work. From Figure 10, it can be seen that the rear steering and VDC torque of the feedforward integration algorithm diverges. The H_∞ control signals are quite large, and sometimes oscillatory (AS moment).

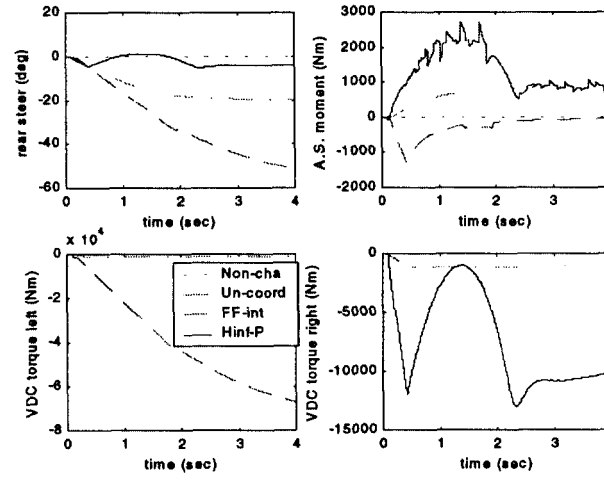

Figure 10 Control inputs under the J-turn with braking maneuver (low mu)

Due to the complexity of the vehicle response, the judgment on the final performance is somewhat subjective. Table 1 summarizes the relative performance of the four vehicles under the scenarios defined in the simulation matrix. Overall, it was found that un-coordinated chassis control only improves slightly from the no-control case, while the H_∞ integrated case was found to perform significantly better. The feedforward integration method works reasonably well when the evaluation maneuver is similar to the case under which the decoupling matrix was obtained. It is possible that a "gain-scheduled" decoupling matrix will work much better. However, we have not fully explored that idea.

Table 1 Summary of vehicle performance

Maneuver	Goal	No Control	Non coordinated	FF Integration	H_∞
Small J	β	4	2	3	1
	$r-r_d$	1	3	4	2
	ϕ	4	1	1	1
Sinusoid	β	4	2	3	1
	$r-r_d$	2	3	3	1
	ϕ	4	2	2	1
J-turn	β	1	3	4	2
	ϕ	4	2	3	1
Fishhook	β	1	3	4	1
	ϕ	3	2	4	1

J with B	β	1	3	4	2
	ϕ	4	2	3	1
J with B Low-μ	β	1	3	4	2
	ϕ	3	1	3	2
Total		37	32	45	19

1: Excellent 2: Good 3: Fair 4:Poor

7. Conclusions

Two types of integrated chassis control design, a feedforward integration and an H_∞ control algorithm, were designed to coordinate the chassis control systems (VDC, 4WS, and active suspension). The performance of the control algorithms was examined using a nonlinear 8DOF (longitudinal, lateral, roll yaw and the rotational motion of the four tires) vehicle model. Simulations were conducted in accordance with a simulation matrix which includes near emergency maneuvers such as J-turn and fishhook on normal as well as low friction surfaces. Performances of the designed integrated controls are summarized as follows:

1. Under non-severe maneuvers, the H_∞ control provides superior performance. The feedforward integration control performs similar or slightly inferior to the un-coordinated control.

2. Under near emergency maneuver conditions (i.e., J-turn and fishhook), the side-slip under the H_∞ control may be worse than the no-control case. This is due to the fact that in severe maneuvers the ABS restricts the torque in order to maintain an appropriate slip ratio.

3. In the low friction case, no controller can change the vehicle behavior while the braking is activated. After the brake is released, all controllers recover the vehicle stability satisfactorily.

Simulation results indicate that the H_∞ control can improve vehicle stability in most situations. If some limitations of inputs are imposed (e.g. by ABS), the improvement reduces significantly.

References

1. Abe, M. et al. (1996), "A Direct Yaw Moment Control for Improving Limit Performance of Vehicle Handling-Comparison and Cooperation with 4WS," *Vehicle System Dynamics* Supplement 25.
2. Allen, R.W. et al. (1992), Vehicle Dynamic Stability and Rollover, DOT HS 807 956.
3. Bender, E.K. (1968), "Optimal Linear Preview Control with Application to Vehicle Suspension," Trans. ASME Journal of Basic Engineering, June, pp.213-221.
4. Garrott, R. et al. (1999), "An Experimental Examination of Selected Maneuvers That May Induce On-road Untripped, Light Vehicle Rollover Phase II of NHTSA's 1997-1998 Vehicle Rollover Research Program," DOT report.
5. Hirano, Y. and E. Ono (1994), "Nonlinear Robust Control And Integrated System of 4WS and 4WD," Proceedings of AVEC'94.
6. Horiuchi, S. et al., (1996), "Two Degree of Freedom H_∞ Controller Synthesis for Active Four Wheel Steering Vehicles," *Vehicle System Dynamics* Supplement 25.
7. Inagaki, S. et al. (1994), "Analysis on Vehicle Stability in Critical Cornering Using Phase-Plane Method," Proceedings of AVEC'94.
8. Ito, M. et al. (1987), "Four Wheel Steering System Synthesized by Model Matching Control," Proceedings of IEE-I Mech 6th International Conference on Automotive Electronics, London.
9. Kitajima, K. (2000), H_∞ Control for Integrated Side-Slip, Roll and Yaw Controls for Ground Vehicles, Master Thesis, University of Michigan.
10. Ma, W. and H. Peng (1998) "Worst-Case Vehicle Evaluation Methodology-Examples on Truck Rollover/Jackknifing And Active Yaw Control Systems," Proceedings of AVEC'98.
11. Mack, J. (1996), ABS-TCS-VDC—Where Will the Technology Lead Us ? SAE PT-57.
12. Matsumoto, S. et al. (1992), "Braking Force Distribution Control for Improved Vehicle Dynamics," Proceedings of AVEC'92.
13. Mauer, G., G. Gissinger, and Y. Chamaillard, (1994), "Fuzzy Logic Continuous and Quantizing Control of an ABS Braking Systems," SAE Paper 940830.
14. Mianzo, L. and H. Peng (1999), "A Unified Hamiltonian Approach for LQ and H_∞ Preview Control Algorithms," *ASME J. of Dynamic Systems, Measurement and Control,* Vol.121, No.3, September 1999, pp.365-369.
15. Nagai, M. and S. Yamanaka (1996), "Integrated Control Law of Active Rear Wheel Steering and Direct Yaw Moment Control," Proceedings of AVEC'96.
16. Sano, S. et al., (1986), "Four-Wheel Steering Systems with Rear Wheel Steer Angle Controlled As A Function of Steering Wheel Angle," SAE Paper 869625.
17. Shibahata, Y. et al. (1992), "The Improvement of Vehicle Maneuverability by Direct Yaw Moment Control," Proceedings of AVEC'92.
18. Shimada, K. and Y. Shibahata (1994), "Comparison of Three Active Chassis Control Methods for Stabilizing Yaw Moments," SAE Paper 940870.
19. Szostak H.T. (1988), "Analytical Modeling of Driver Response In Crash Avoidance Maneuvering-Volume II: An Interactive Tire Model For Driver/Vehicle Simulation" DOT HS 807 271.
20. Tagawa, T. et al. (1996), "A Robust Active Front Wheel Steering System Considering the Limits of Vehicle Lateral Force," Proc. of AVEC'96.
21. Tan, H.S. and M.Tomizuka (1990), "An Adaptive Sliding Mode Vehicle Traction Controller Design," Proceedings of the American Control Conference, San Diego, California.
22. Thompson, A.G. (1976), "An Active Suspension with Optimal Linear State Feedback," *Vehicle System Dynamics.*
23. Van zanten, A.T. et al. (1996), "Control Aspects of The Bosch-VDC," Proceedings of AVEC'96.
24. Whitehead, J.C. (1988), "Four Wheel Steering: Maneuverability and High Speed Stabilization," SAE Paper 880642.